Neutron-proton and neutron-neutron quasifree scattering in the *n-d* breakup reaction at 26 MeV

A. Siepe, J. Deng,* V. Huhn,† L. Wätzold,‡ Ch. Weber,§ and W. von Witsch‖
Institut für Strahlen und Kernphysik, Universität Bonn, D-53115 Bonn, Germany

H. Witała
Institute of Physics, Jagellonian University, Reymonta 4, PL-30059 Cracow, Poland

W. Glöckle
Institut für Theoretische Physik II, Ruhr-Universität Bochum, D-44780 Bochum, Germany
(Received 10 September 2001; published 4 March 2002)

The regions of neutron-proton and neutron-neutron quasifree scattering (QFS) have been investigated in the *n-d* breakup reaction at 26 MeV, measuring absolute cross sections with an accuracy of a few percent. The data were analyzed by means of detailed Monte Carlo simulations based on rigorous three-body calculations with realistic nucleon-nucleon potentials. For *n-p* QFS, good agreement between theory and experiment was found. In contrast, for *n-n* QFS the experimentally determined cross section is almost 20% larger than the theoretical predictions.

DOI: 10.1103/PhysRevC.65.034010 PACS number(s): 13.75.Cs, 21.45.+v, 25.10.+s

I. INTRODUCTION

Quasifree scattering (QFS) represents a prominent kinematical situation in three-body breakup reactions. Similar to the final-state interaction (FSI), in quasifree scattering the spectrum has a distinctive structure; the cross section is large and is characterized by a pronounced peak where the energy of the spectator particle reaches a minimum.

One of the most interesting reactions in this regard is the neutron-induced breakup of the deuteron. There are only three nucleons in this system, two of which are neutrons. Because there are no Coulomb forces acting, dynamically exact Faddeev-type calculations [1] can be performed with realistic nucleon-nucleon (*N-N*) interactions, making neutron-neutron QFS in the $^2\mathrm{H}(n,nn)p$ reaction an important tool for the investigation of the *n-n* interaction. However, not many high-quality data exist for either *n-n* or *n-p* QFS, for obvious reasons: since, at the exact quasifree point, the spectator proton does not produce a signal in the target, one either has to move away from the ideal kinematics, or the experiment must be performed without a target signal, which requires a pulsed or tagged neutron beam and provokes a large accidental background; for *n-p* QFS to be studied in the same reaction, a thin target must be used, necessitating a very intense neutron beam.

In most of the previous *n-d* breakup experiments investigating *n-n* QFS, the stated aim [2] was to exploit the apparent strong dependence of the cross section upon the effective range in order to determine r_{nn}, either by measuring the absolute value of the *n-n* cross section [3,4] or some relative quantity, such as the ratio of $\sigma(n\text{-}n)/\sigma(n\text{-}p)$ [5]. In the meantime, however, it has been found that this is not possible because r_{nn} is *not* an independent parameter [6]. The only quantity that can be adjusted within the framework of any given interaction model is the scattering length a_{nn} (whose effect on the QFS cross section is small). Once a_{nn} is given, r_{nn} is essentially fixed and cannot be changed at will. Furthermore, its value is virtually the same for any modern, realistic *N-N* potential [7–9] and, because $\Delta r_{nn} = 0.017\Delta a_{nn}$ [6], even changing a_{nn} drastically would have little effect on r_{nn}. Nevertheless, *n-n* QFS is still an interesting problem because it probes the neutron-neutron interaction and allows to test the reliability of present-day three-body calculations. In this paper we report on two experiments in which *n-n* and *n-p* QFS were investigated at 26 MeV using the *n-d* breakup reaction.

II. EXPERIMENTAL DETAILS

A. Experimental setup

The experiments were performed at the cyclotron laboratory of the Institut für Strahlen- und Kernphysik at the University of Bonn. Since the setup and procedure were basically the same as in several previous experiments [10] in which the *n-n* and *n-p* FSI were investigated, only a short synopsis will be given here.

The neutron beam was produced *via* the $^2\mathrm{H}(d,n)^3\mathrm{He}$ reaction with 27.3 MeV deuterons incident on a 47-mm-long, liquid nitrogen cooled gas target, operated at a pressure of 40 bars. The primary beam was stopped directly behind the gas target that served as a Faraday cup. The neutrons were collimated at 0° in a 120-cm-long W-Cu collimator to form a well-defined circular beam with a diameter of 31 mm (full width at half maximum) at the reaction target, which was positioned 195 cm from the center of the gas target. At a

*Permanent address: Department of Nuclear Physics, China Institute of Atomic Energy, Beijing, People's Republic of China.
†Present address: Deutsche Telekom MobilNet GmbH, D-53123 Bonn, Germany.
‡Present address: AMD Saxony Manufactoring, D-01330 Dresden, Germany.
§Present address: Arcor AG & Co., D-65760 Eschborn, Germany.
‖Electronic address: vwitsch@iskp.uni-bonn.de

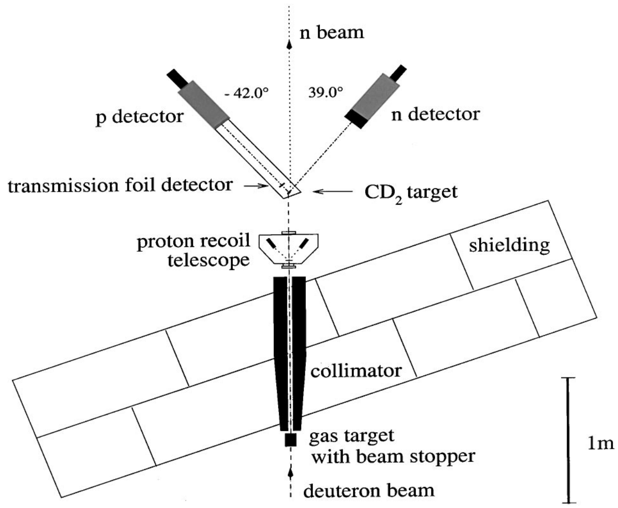

FIG. 1. Schematic drawing of the experimental setup for the measurement of quasifree *n-p* scattering. For *n-n* QFS, the proton arm was replaced by a second neutron detector.

deuteron beam intensity of 200 nA, the neutron flux on the target in the quasimonoenergetic high-energy (HE) peak from the $^2H(d,n)^3He$ reaction was $3.7\times10^5\ s^{-1}$, with an average energy $E_0=26$ MeV and an energy spread $\Delta E_0=4.0$ MeV. The HE neutrons could be separated cleanly from the lower-energy (LE) breakup continuum of the $^2H(d,n)pd$ reaction by their time of flight (TOF). As a beam monitor, a double proton-recoil telescope (PRT) was placed in the *n* beam 148 cm from the gas target to detect protons emitted from a 24-mg/cm^2-thick CH_2 target at angles of $\pm35°$ with respect to the *n* beam. The PRT was used for the absolute normalization of the HE neutron beam as described in Sec. II B.

A schematic view of the experimental layout for the measurement of *n-p* QFS is shown in Fig. 1. The neutrons were detected at $\Theta_n=39°$ and protons at $\Theta_p=42°$, with $\phi_{np}=180°$. The angle Θ_n was chosen to be 3° from the exact symmetric QFS position to assure that no elastic *n-p* coincidences from the 1% hydrogen contamination in the deuterium target could reach the detectors. The reaction target was a deuterated polyethylene foil with a thickness of 34 mg/cm^2, suspended in an Al frame by means of two thin Be wires. It had an elliptical shape and was oriented such that it faced the proton detector, thereby appearing to the neutron beam as a circular disc with 22 mm diameter. At the position of the CD_2 target, the *n* beam had a plateau of constant intensity with a diameter of greater than 25 mm so that the whole target was illuminated homogeneously. At a distance of 8 cm from the target and outside of the neutron beam, an NE104 scintillator foil of 4.7 mg/cm^2 thickness was positioned in an Al reflector equipped with thin entrance and exit foils, viewed from above by a photomultiplier. The signals produced by charged particles in this transmission foil detector (TFD) were used as start signals for all TOF measurements. The protons were detected with a plastic scintillator of 10 cm diameter and 5 mm thickness that was positioned 70 cm from the CD_2 target and viewed by a 5 in photomultiplier. The target and transmission detector were mounted in an evacuated pipe, in the following called "proton arm," which was sealed at the front end with a Be entrance window and a Ti exit foil for the *n* beam. At the far end it was closed by the *p* detector. The *n* detector was positioned at a distance of 75 cm from the CD_2 target on the opposite side of the beam axis. It had a nominal diameter of 5 in and a thickness of 3 in and was equipped with *n*-γ pulse-shape discrimination. All detectors were unshielded and surveyed to a precision of less than 0.05°. They were provided with LED pulsers to monitor gain shifts, dead times and pileup.

For the *n-n* measurement, the proton arm was replaced by a second *n* detector of equal size. Both *n* detectors were positioned symmetrically at $\Theta_n=42°$ and placed 75 cm from the target, which now consisted of a thin-walled, upright Al cylinder that had a height of 65 mm and a diameter of 44 mm and was filled with C_6D_{12} liquid scintillator. It was closed at the bottom with a quartz window and viewed from below by a photomultiplier.

B. Calibrations and efficiencies

The neutron fluence F_n in the intensity plateau of the beam was measured by means of *n-p* scattering. For this, the CD_2 target in the proton arm was replaced by a 10-mg/cm^2 CH_2 foil of equal size. Knowing the number of hydrogen atoms in the target, the *n-p* cross section, and the solid angle of the *p* detector, the number of neutrons/cm^2 could then be calculated from the number of recoil protons detected. A second, independent value for F_n was obtained from the simultaneous PRT measurement. Taking both measurements together, the integrated HE neutron flux for the subsequent measurements with the CD_2 target could, thus, be determined with an absolute accuracy of 1.1%, using the PRT as a relative monitor.

The beam-target luminosity *BT* for the *n-n* measurement was also determined through *n-p* scattering. For this purpose the C_6D_{12} target cylinder was replaced by an identical one filled with C_6H_6. Scattered neutrons were detected at $\Theta_n=42°$, and the integrated luminosity was determined relative to the number of counts in the PRT. In fact, this measurement at once provided the product of $(BT\times\varepsilon\times\triangle\mathbf{\Omega})$, where ε and $\triangle\mathbf{\Omega}$ are the efficiency and the solid angle of the *n* detector, respectively. The luminosity was also *calculated* with a detailed Monte Carlo (MC) simulation based on the accurately known value of F_n. Both results for *BT* agreed within 0.6%, and the overall error for this quantity is estimated to be 1.2%.

The efficiency of the transmission foil detector was determined with the same setup as described above. By comparing the number of protons counted with and without a coincident TFD signal, the efficiency of the transmission detector was found to be practically 100% at all proton energies.

The efficiency of the *n* detectors was determined in two steps. First, the *central* efficiency was measured, using again the setup with the CH_2 target. The *n* detector was positioned at 90° with respect to the proton arm and close to the target to assure that all *n-p* neutrons hit the detector near its center in a narrow cone defined by the solid angle of the *p* detector. The whole spectrum of the neutron beam was used, including the continuum from the $^{2}H(d,n)pd$ reaction, so that the efficiency could be determined simultaneously for all energies between $E_n = 2.7$ and 11 MeV. Windows were set offline in the TOF spectrum of the incoming neutron beam to select bins of energies for the scattered neutrons for which the efficiency was then determined from the number of free proton counts vs the number of *p-n* coincidences. The results were compared with MC calculations based on an expanded version [11] of the PTB Monte Carlo efficiency program developed by Dietze and Klein [12], and the agreement was very good for all energies [10]. The main advantages of this measurement were that the efficiency was determined *in situ*, with the same setup and under virtually the same conditions that existed in the breakup experiment, and that it was a relative measurement. Thus, beam attenuation from the gas target to the detector was of no concern and the change in the efficiency due to pileup, which is quite important at high count rates, was automatically included. Therefore, apart from the fact that edge effects were not present here, the results could be applied directly to the breakup experiment. The main error in this measurement was due to statistics, and we conclude that the PTB-based calculations, when renormalized to the experimental results, reproduce the central efficiency of our *n* detectors within $\pm 0.9\%$ in the whole energy range measured.

In order to obtain the *average* efficiency ε as needed for the *n-d* breakup experiments, the PTB program was employed again to allow for edge effects, which can be calculated very accurately. The additional error in the deduced average efficiency is not larger than 1%, resulting in a total error for ε of $\pm 1.4\%$ [10]. The PTB program also provided the radial dependence of ε.

C. Data acquisition and reduction

For the measurement of *n-p* QFS, the event trigger signal was generated by a fast coincidence among the TFD, *p* detector, and the *n* detector. For each trigger, eight experimental parameters were written to the disc in list mode: the dynode signal as well as (for pulse-shape discrimination purposes) the long and short components of the anode signal from the *n* detector, the dynode signals from the TFD and from the *p* detector, and the TOF's between the TFD and the *n* detector (TOF_n), the *p* detector (TOF_p), and the rf of the cyclotron (TOF_C), respectively. Besides, twofold coincidences were recorded between the $\triangle E$ and E detectors of the PRT. The trigger signals from the LED pulser driver were counted with a scaler and used to create a separate gate.

In the *n-n* QFS experiment a different strategy had to be used. Since the two *n* detectors were placed at the exact QFS angles, most of the spectator protons did not produce a usable signal in the target scintillator. Consequently, only twofold coincidences could be required between the two *n* detectors, and the energy of the neutrons was measured via their TOF with respect to the rf of the cyclotron. In addition, the time between the signals in the two *n* detectors, TOF_{12}, was measured to allow for the subtraction of accidental background, while the signals from the target were used for diagnostic purposes only.

The total effective running time of the two experiments was approximately 350 h, divided into five blocks of 1 week each. The beam intensity was 850 and 140 nA for *n-p* and *n-n* QFS, respectively. It was adjusted such as to keep the number of accidentals in each case at about 15%. The singles count rates for the *n-p* measurement were 2 kHz in the TFD, 10 kHz in the *p* detector, and 85 kHz in the *n* detector while the corresponding rates in the *n-n* experiment were 280 kHz in the target and 10 kHz in the *n* detectors. Special care was taken to limit fluctuations in the count rate of the *n* detectors to less than $\pm 6\%$; the data acquisition system was stopped automatically when this limit was exceeded. A background run was made in the *n-p* measurement with the CD_2 target replaced by a CH_2 target of equal thickness in order to investigate possible contributions from the small (1%) hydrogen contamination in the CD_2 foil; however, no true coincidences were observed in the region of interest. In the *n-n* measurement, another background run was carried out in which the target was replaced by a carbon cylinder of equal size. Because of the large negative *Q*-value of the $^{12}C(n,nn)^{11}C$ reaction there could be no true coincidences from carbon, but the TOF_{12} spectrum revealed that the number of counts in the "prompt" peak was about 20% larger than in the "accidental" ones. These counts were mostly due to $^{14}N(n,nn)^{13}N$ reactions in the air, which in effect constituted a fairly thick target for the neutron beam. Another contribution came from cross talk where a neutron would undergo multiple scattering in one of the detectors and then be seen by the other one. Altogether, however, under the conditions applied in the analysis, these kinds of "true" backgrounds accounted for only 2% of all real coincidences in the *n-n* QFS measurement.

For *n-p* scattering, the raw data were first reduced by selecting the HE part of the *n* beam. A lower threshold equivalent to 60 keV electron energy (keVee) was set in the dynode spectrum of the *n* detector. Then, a window was set in the pulse-shape matrix to get rid of most coincidences with γ rays in the *n* detector. Coincidences with deuterons in the *p* detector were removed by an appropriate window in the (E_p vs TOF_p) matrix. In all cases, conservative windows were used to assure that no true coincidences were lost in the process. The remaining background, being accidental, was subtracted in the usual way after projection onto the TOF_n axis. For *n-n* scattering, thresholds of 1 MeV electron energy (MeVee) were required for the dynode signals of the *n* detectors, corresponding to a neutron energy of roughly 3 MeV, in order to remove the ambiguities caused by the 28-MHz repetition rate of the rf signal from the accelerator. Accidentals were eliminated using TOF_{12} as described above, and the small contributions from the $^{14}N(n,nn)^{13}N$ reaction and from cross talk were subtracted after proper normalization. In addition, the analysis was repeated with thresholds of 1.5 MeVee.

D. Data analysis and corrections

Some corrections were applied to the reduced data prior to their comparison with theory. Long-time gain changes in the photomultipliers and small shifts of the time-zero points were corrected by means of the pulser peaks that were recorded in all spectra together with the *n-d* data. Also, each TOF was corrected for residual walk as explained in [10]. All other distorting effects were included in the Monte Carlo simulations of the experiments.

One of the most important corrections was, of course, the efficiency of the *n* detectors that was taken from the renormalized PTB calculations described above. The radial dependence of ε was taken into account explicitly. For *n-p* QFS, other effects besides the extended geometry included the energy spread of the beam, the time resolution, straggling and energy loss of the protons, and the loss of neutrons due to scattering that, however, was very small. Owing to the high count rate in the *n* detector, there was a probability of around 2% for any TOF in the neutron arm to be stopped early by an accidental count, thus leading to an apparent loss of true coincidences by moving the event to the left on the time axis, towards and into the "accidentals region," which consequently became somewhat contaminated by true coincidences. Reverting to the measured distribution of pulser counts along the TOF_n axis, the exact magnitude of the necessary correction was calculated for each event. The number of recorded pulser coincidences also served to determine the overall dead time losses, which were 0.6%.

For the data of the *n-n* measurement the most important correction—apart from the efficiency—was due to multiple scattering in the target. As calculated from the total cross sections for carbon and deuterium, 17.0% of the incoming neutrons were scattered before inducing a reaction, while the probability for scattering of either one of the breakup neutrons was 19.5%, resulting in a total loss of 46.2%. However, by simulating the effects of double scattering individually it was found that some of those events that scattered before the breakup reaction actually did contribute to the count rate in the QFS peak. Also taken into account explicitly was the possibility that one of the breakup neutrons, being first emitted in an arbitrary direction, might be detected after scattering in the target. Together, these effects led to an increase in the count rate of 3.0%, which shows that double scattering in a thick target must be investigated carefully and cannot, in general, be treated summarily. Overall, the corrections for the *n-n* data were substantial. However, they are all well understood and can be made very accurately.

Absolute theoretical spectra were produced with $3N$ breakup cross sections obtained from rigorous, fully charge-dependent Faddeev-type calculations in momentum space that used the CD-Bonn potential [9] as input for the *N-N* interaction. A detailed description of the theoretical formulation and numerical procedure can be found in Ref. [1] and will not be repeated here. The CD-Bonn interaction is charge dependent in the isospin $t=1$ states, taking the difference in the ${}^1S_0$-force components of the *n-n* and *n-p* subsystems explicitly into account. This potential is "realistic" in that it describes the existing $2N$ data with a normalized $\chi^2 \approx 1$. Point-geometry cross sections were calculated for energies from 23 to 28 MeV in steps of 0.5 MeV, and stored in the computer. From this library, the cross section was interpolated for each simulated event and incorporated into the Monte Carlo routine [13]. The mesh points were so chosen

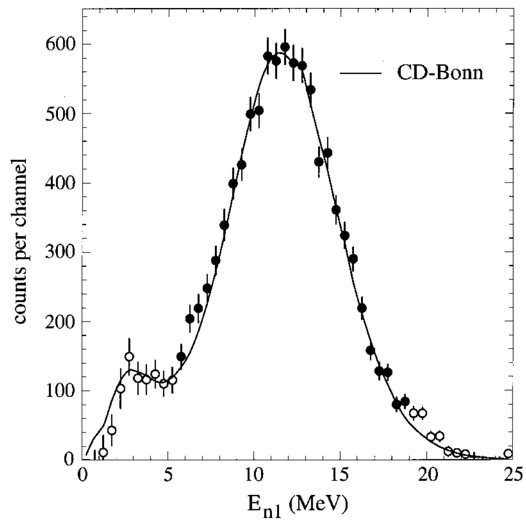

FIG. 2. Data for *n-p* QFS, projected onto the E_n axis. The solid line is the finite-geometry Monte Carlo prediction, using CD-Bonn for the *N-N* interaction.

as to assure that the interpolated cross section in no case deviated from the exact value by more than 0.1%. (For the simulation of multiple scattering, where cross sections were needed over a much larger angular range, a coarser grid was used.) Finally, the measured number of counts in the QFS peak was compared with the corresponding predicted numbers. In addition to CD-Bonn, the cross section calculations were repeated with three other realistic *N-N* potentials [7,8].

The possible effect of a three-nucleon force (3NF) was estimated by adding the Tucson–Melbourne 3NF to the *N-N* interactions; a brief outline of the procedure and further references are given in Ref. [14]. However, the resulting changes in the peak cross sections were less than 0.3% for *n-p* QFS and 0.6% for *n-n* QFS.

III. RESULTS

A. Neutron-proton QFS

The final data for *n-p* QFS, with their statistical errors, are shown in Fig. 2, after conversion of the neutron TOF to energy and projection onto the E_n axis. Included is the finite-geometry Monte Carlo prediction using CD-Bonn for the *N-N* interaction. The projection on E_n was chosen in order to avoid distortions caused by the energy smearing in the target. The theory reproduces the measurement absolutely within 1.8%. Only the dark points in Fig. 2 were used for the comparison because the data in the wings of the peak are either close to the threshold of the *n* detector, or the proton energies are very low. The overall statistical accuracy is 1.2%. To this must be added an error of 1.4% from the efficiency of the *n* detector, 1.1% from the fluency of the *n* beam, 0.9% and 0.8% for the solid angles of the *n* and *p* detectors, respectively, and 0.5% for other effects including geometry, resulting in a total experimental error of 2.5%. Thus, for *n-p* QFS the theoretical prediction agrees with the measured cross section within $(1.8\pm2.5)\%$. Using any of the other *N-N* potentials instead of CD-Bonn changes the result by less than 1%. The shape of the peak is also reproduced well, with $\chi^2{}_{\mathrm{min}}$

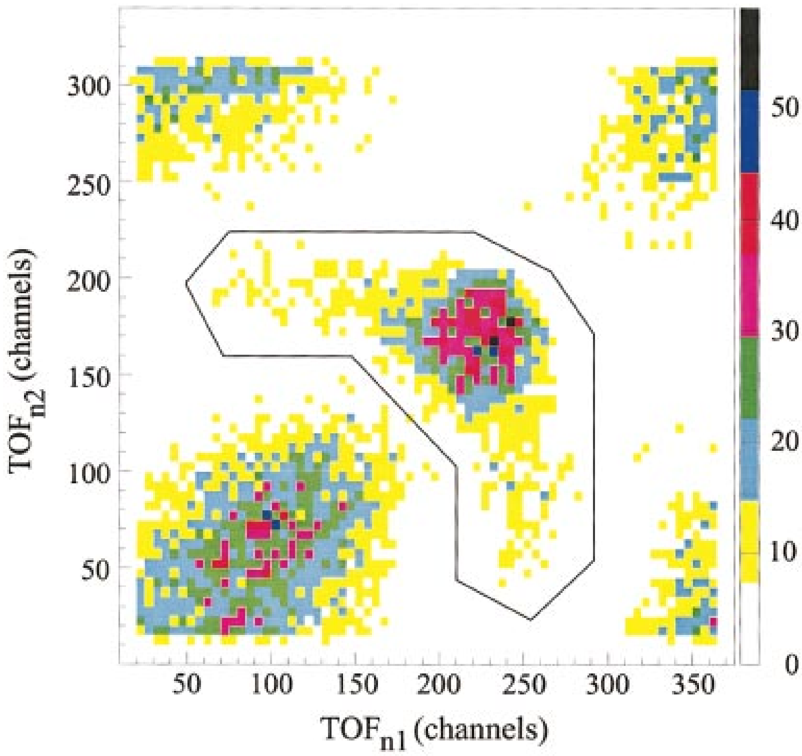

FIG. 3. (Color) The matrix (TOF$_{n1}$ vs TOF$_{n2}$) for n-n QFS. Gamma coincidences have been removed by pulse-shape analysis, and thresholds corresponding to 1 MeVee were applied in the dynode spectra of the n detectors. Increasing channel numbers correspond to shorter flight times. The boomerang-shaped area in the center is the kinematical locus populated by coincidences from the HE part of the n beam; further explanations are given in the main text.

=25 for 24 degrees of freedom (DOF). Essentially the same result was obtained in a previous experiment by Huhn *et al.* [10] where the n-p quasifree peak was observed together with the n-n final-state interaction.

B. Neutron-neutron QFS

The data for n-n QFS are depicted in matrix form in Fig. 3 where TOF$_{n2}$ is plotted vs TOF$_{n1}$, after gammas have been eliminated by pulse-shape analysis and thresholds corresponding to 1 MeVee applied in the dynode spectra of the n detectors, as detailed in Sec. II C; here, increasing channel numbers correspond to smaller flight times. The visible time window on each axis corresponds to 35.6 ns, which is the time between two stop signals from the rf of the cyclotron. The boomerang-shaped area in the center is the kinematical locus populated by coincidences from the HE part of the n beam, while in the lower left-hand corner events from the LE part of the beam are seen. In the other three corners, LE events appear, which are displaced by 35.6 ns. The spectrum is rather clean, and the HE and LE regions are clearly separated from each other. In Fig. 4, the HE data are shown projected onto the E_{n1} axis, after subtraction of background. An additional software threshold of 6 MeV has been applied in E_{n2} to eliminate events with energies close to the detection threshold; for the same reason, the data represented by open circles have not been included in the analysis. The projection on the same energy axis as in Fig. 2 was chosen to facilitate the comparison with the n-p data.

From Fig. 4 it is immediately apparent that there is a large discrepancy between the experimentally measured yield and the MC prediction, represented by the solid line. As in the n-p case, the shape of the peak is well described, as indicated by the dotted curve, which is the MC calculation normalized to the experiment (χ^2 per DOF=0.9). However, the absolute yield is underestimated by (17.8±3.2)% using CD-Bonn [9], and by 19.5% with the Argonne v_{18} potential [8]; the results based on the Nijmegen I and II potentials [7] are very close to CD-Bonn. Increasing the absolute value of the n-n scattering length a_{nn} by 1 fm increases the QFS cross section by 1.5%. The total experimental error of 3.2% (one standard deviation) is due to statistics (1.2%), uncertainties in the background subtraction (1.0%), the solid angle $\Delta\mathbf{\Omega}_1$ of the first n detector (0.9%), the efficiency ε_1 of this detector (1.4%), the neutron attenuation factor (1.5%), uncertainties

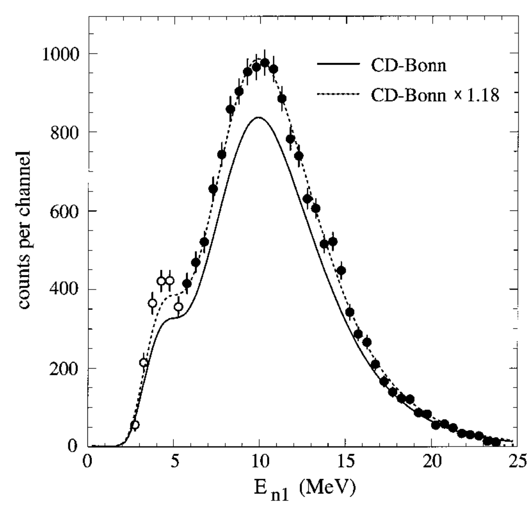

FIG. 4. HE data of Fig. 3, projected onto the E_{n1} axis. The solid curve represents the finite-geometry Monte Carlo prediction using CD-Bonn, the dotted line is the MC result normalized to the experiment by multiplication with a factor of 1.18. Only events with E_{n1} and E_{n2}>6 MeV have been included in the analysis.

in the geometry (0.3%) and, finally, the product of $(BT\times\varepsilon_2\times\triangle\mathbf{\Omega}_2)$, which contributes 1.6% (see Sec. II B and Ref. [10]). The results are essentially the same with dynode thresholds of 1.5 MeVee instead of 1.0 MeVee, the discrepancy (using CD-Bonn) then being 18.6% instead of 17.8%.

After these results had become apparent, the *n-n* measurement was repeated with a different setup. For this, the neutron detectors were positioned at a distance of 45 cm from the target at the asymmetric angle pair $\Theta_{n1}=32°$, $\Theta_{n2}=52°$, and $\Phi=180°$. Also, a smaller target was used that now consisted of a 20-mm-long CD_2 cylinder with a diameter of 20 mm, thereby reducing multiple-scattering effects considerably. It was oriented with its axis pointing in the beam direction, and situated completely within the plateau of constant beam intensity so that the luminosity *BT* was determined directly by the count rate in the PRT, as in the *n-p* measurement. Again, a background run was made with the CD_2 target replaced by a carbon cylinder of equal size. After the new QFS data were taken, the efficiency of the *n* detectors was measured again at one energy ($E_n=7$ MeV) by way of *n-p* scattering, this time using only the HE part of the neutron beam. Recoil protons emitted from a small CH_2 target were detected at 32° with a Si surface barrier detector, placed at a distance of 10 cm from the target and operated in air. The efficiency of the two *n* detectors was found to agree with the previously determined value [10] within $(-1.6\pm3.7)\%$. The data of this second *n-n* QFS measurement were analyzed by means of Monte Carlo simulations as before. The new results fully confirmed the previous ones, the measured yield this time exceeding the CD-Bonn prediction by $(18.4\pm3.9)\%$.

IV. DISCUSSION

Considering the perfect agreement between data and theory for *n-p* QFS (see also the corresponding results in Ref. [10]), the large difference found in the *n-n* experiment is surprising, the disagreement corresponding to more than five standard deviations. In this context, it should be noted that the first of the two *n-n* QFS measurements was sandwiched between two other experiments whose results were in full agreement with the theoretical predictions: immediately preceding it, the *n-p* scattering length was measured using *exactly the same setup* [10]; in this experiment, the well-known value of a_{np} was reproduced nicely, the difference between the predicted and the measured yield being only $(0.5\pm3.7)\%$. Similarly, the *n-p* QFS measurement was performed right *after* the first *n-n* experiment. Thereby, many sources of errors are essentially ruled out as a possible explanation for the disagreement observed in the *n-n* QFS case. In addition, of course, there is the virtually identical result of the second *n-n* measurement.

Unfortunately, quasifree scattering in *p-d* breakup, for which several accurate experiments have been performed [15], cannot be used for comparison because of Coulomb effects that are appreciable in the region of QFS [16], and *p-d* calculations with a realistic nuclear input are not yet available. Also, a look at most previous *n-d* measurements [3–5,17,18] is of little help because the experimental uncertainties were large, and rather primitive calculations were used for the analysis.

To our knowledge, there is only one more *n-d* experiment in which *n-n* QFS was investigated with reasonable accuracy and compared with rigorous breakup calculations [19,20]. In this experiment, which was performed at a bombarding energy of 10.3 MeV, several angles were measured, using two different setups. Interestingly, here the experimental cross sections were also found to be significantly higher than the theoretical predictions—on average by about 13%. Although the analysis of this experiment was performed with three-body calculations using the older, less realistic Paris [21] and Bonn-*B* [22] potentials as input for the *N-N* interaction, the results are essentially the same if the cross sections are calculated with the more modern potentials [7–9]. Therefore, this experiment [19] appears to corroborate our own results, suggesting that the *n-d* breakup cross section in the region of *n-n* QFS is not predicted correctly by the theory. There are other kinematical situations where this is the case, most notably the so-called ‘‘space star’’ geometry where the measured cross sections are some 25% higher than the predicted ones [23]. However, in order to definitely confirm this new ‘‘puzzle’’ in three-nucleon physics, an additional, independent high-precision measurement of neutron-neutron quasifree scattering is called for.

ACKNOWLEDGMENTS

We would like to thank Dipl. Phys. J. Graichen for his help during the second neutron-neutron QFS experiment. This work was supported by the Deutsche Forschungsgemeinschaft under Grant No. WI 1144/5-2, and by the Polish Committee for Scientific Research under Grant No. 2P03B02818. The three-body calculations were performed on the CRAY T90 and T3E of the John von Neumann Institute for Computing in Jülich, Germany.

[1] H. Witała, Th. Cornelius, and W. Glöckle, Few-Body Syst. **3**, 123 (1988); H. Witała, W. Glöckle, and Th. Cornelius, Phys. Rev. C **39**, 384 (1989); W. Glöckle, H. Witała, D. Hüber, H. Kamada, and J. Golak, Phys. Rep. **274**, 107 (1996).
[2] I. Šlaus, Y. Akaishi, and H. Tanaka, Phys. Rep. **173**, 267 (1989).
[3] J. Soukup, J. M. Cameron, H. W. Fielding, A. H. Hussein, S. T. Lam, and G. C. Neilson, Nucl. Phys. **A322**, 109 (1979).
[4] H. Guratzsch, B. Kühn, H. Kumpf, J. Mösner, W. Neubert, W. Pilz, G. Schmidt, and S. Tesch, Nucl. Phys. **A342**, 239 (1980).
[5] W. von Witsch, B. Gómez Moreno, W. Rosenstock, R. Franke, and B. Steinheuer, Nucl. Phys. **A346**, 117 (1980).
[6] R. Machleidt (private communication).
[7] V. G. J. Stoks *et al.*, Phys. Rev. C **49**, 2950 (1994).
[8] R. B. Wiringa, V. G. J. Stoks, and R. Schiavilla, Phys. Rev. C **51**, 38 (1995).

[9] R. Machleidt, F. Sammarruca, and Y. Song, Phys. Rev. C **53**, 1483 (1996).
[10] V. Huhn, L. Wätzold, Ch. Weber, A. Siepe, W. von Witsch, H. Witała, and W. Glöckle, Phys. Rev. C **63**, 014003 (2001).
[11] I. Fabry, Diplom thesis, University of Bonn, 1998.
[12] G. Dietze and H. Klein, Physikalisch-Technische Bundesanstalt Braunschweig, Technical Report PTB-ND-22, 1982; G. Dietze and H. Klein, Nucl. Instrum. Methods Phys. Res. **193**, 549 (1982).
[13] L. Wätzold, Ph.D. thesis, University of Bonn, 2000.
[14] P. Hempen, P. Clotten, K. Hofenbitzer, T. Köble, W. Metschulat, M. Schwindt, W. von Witsch, W. Glöckle, D. Hüber, and H. Witała, Phys. Rev. C **57**, 484 (1998).
[15] H. Patberg, R. Großmann, G. Nitzsche, L. Sydow, S. Vohl, H. Paetzgen Schieck, J. Golak, H. Witała, W. Glöckle, and D. Hüber, Phys. Rev. C **53**, 1497 (1996), and references therein.
[16] E. O. Alt and M. Rauh, Few-Body Syst. **17**, 121 (1994).
[17] I. Slaus, J. W. Sunier, G. Thompson, C. J. Young, J. W. Verba, D. J. Margaziotis, P. Doherty, and R. T. Cahill, Phys. Rev. Lett. **26**, 789 (1971).
[18] E. Bovet, F. Foroughi, and J. Rossel, Nucl. Phys. **A304**, 29 (1978).
[19] W. Lübcke, Ph.D. thesis, University of Bochum, 1992.
[20] J. Krug (private communication).
[21] M. Lacombe, B. Loiseau, J. M. Richard, R. Vinh Mau, J. Coté, P. Pirés, and R. de Tourreil, Phys. Rev. C **21**, 861 (1980).
[22] R. Machleidt, Adv. Nucl. Phys. **19**, 189 (1989).
[23] C. R. Howell *et al.*, Nucl. Phys. **A631**, 692c (1998), and references therein.